Journal of Power Sources 195 (2010) 1344–1351

Contents lists available at ScienceDirect

Journal of Power Sources

journal homepage: www.elsevier.com/locate/jpowsour

Carbon deposition on Ni/YSZ anodes exposed to CO/H_2 feeds

Vanesa Alzate-Restrepo, Josephine M. Hill*

Department of Chemical and Petroleum Engineering, University of Calgary, 2500 University Dr NW, Calgary, Alberta T2N 1N4, Canada

ARTICLE INFO

Article history:
Received 13 July 2009
Received in revised form 3 September 2009
Accepted 4 September 2009
Available online 13 September 2009

Keywords:
Solid oxide fuel cells
Carbon deposition
Ni/YSZ
Carbon monoxide
Hydrogen
Deactivation

ABSTRACT

Solid oxide fuel cells (SOFC) can be operated with a variety of fuels. In anode-supported SOFC, these fuels may decompose or react catalytically in the anode compartment resulting in mixtures that, in most cases, include high concentrations of H_2 and CO. In this study, the formation of carbon from CO and H_2 mixtures on Ni/YSZ anodes at 1073 K has been investigated using electrochemical and carbon characterization techniques. More carbon is deposited when Ni/YSZ anodes are exposed to CO/H_2 mixtures than to pure CO. Polarization of the anodes reduced the amount of carbon deposited but the extent of the reduction depended on the gas composition.

1. Introduction

Solid oxide fuel cells (SOFC) have the potential of converting traditional and alternative fuels to power more efficiently than conventional energy conversion devices. Prospective fuels for SOFC include natural gas, propane, gasoline, diesel, methanol, ethanol, and products of the gasification of coal and biomass [1]. SOFC operate at temperatures between 900 and 1273 K in order for the solid electrolyte (typically yttria-stabilized zirconia, YSZ) to have sufficient conductivity. At these high temperatures, hydrocarbon and alcohol fuels may decompose in the gas-phase, react catalytically, or be reformed by steam in the anode compartment. The products of these reactions are predominantly hydrogen (H_2) and carbon monoxide (CO) with some other species that depend on the initial feed. For example, according to thermodynamic calculations, at 1073 K methanol decomposes in the gas-phase to 63% H_2 and 30% CO, while ethanol decomposes to 71% H_2 and 22% CO (the balance in the gas-phase includes CO_2, CH_4, and H_2O for both methanol and ethanol) [2]. The steam gasification of coal can produce a stream that contains 30% H_2 and 60% CO [3], while biomass gasification may produce a mixture with 17% H_2 and 13% CO [4].

These reaction streams can be electrochemically oxidized at the anode in an SOFC according to Eqs. (1) and (2) for H_2 and CO, respectively.

$$H_2 + O^{-2} \rightarrow H_2O + 2e^- \quad (1)$$

$$CO + O^{-2} \rightarrow CO_2 + 2e^- \quad (2)$$

SOFC anodes typically contain nickel, which is a very active material for the formation of carbon deposits [5,6]. For alkane-based fuels (e.g., methane, propane, and butane), carbon formation occurs through reactions (3)–(5). The extent of each reaction and the type of carbon deposited depends on the temperature and gas composition. For example, carbon produced by methane decomposition produces predominantly carbon fibres at temperatures below 873 K, while at higher temperatures, carbon diffuses through the nickel particles causing severe swelling [7].

$$C_nH_{2n+2} = nC + (n+1)H_2 \quad (3)$$

$$2CO = C + CO_2 \quad (4)$$

$$CO + H_2 = C + H_2O \quad (5)$$

Because carbon formation is a problem for catalytic applications such as reforming and methanation, and for corrosion of high temperature systems, this problem has been widely studied on supported nickel catalysts and nickel foils [5,6,8–18]. In the catalytic systems, the nickel particles are dispersed on a porous support [9] and have diameters on a nanometre scale, and the reaction temperatures are typically around or below 873 K. Since carbon fibres and filaments are formed at these conditions, there is a vast literature relating carbon formation on nickel with carbon nanotubes and fibres [9,11,19,20]. Therefore, there is the misconception that carbon forms fibres or filaments at all conditions.

In corrosion studies, nickel is present as a foil and the exposure temperature range is broad. The formation of carbon is known as metal dusting since the carbon disintegrates the metal into powder

* Corresponding author. Tel.: +1 403 210 9488; fax: +1 403 284 4852.
E-mail address: jhill@ucalgary.ca (J.M. Hill).

0378-7753/$ – see front matter © 2009 Elsevier B.V. All rights reserved.
doi:10.1016/j.jpowsour.2009.09.014

[21]. For other metals susceptible to this type of corrosion, the formation of carbides is a necessary step in the process [21]. This step is only relevant for nickel at low temperatures because nickel carbide decomposes in the region of 573–723 K [13]. Carbon on nickel forms graphite directly at higher temperatures, causing metal dusting. The nickel becomes dust due to the presence of graphite inside the metal structure, which forms as the carbon diffuses through the nickel [17].

More recently, carbon deposition has become a research area for SOFC fuelled by hydrocarbons [7,9,22–29]. For SOFC anodes, however, the system is different from corrosion and conventional heterogeneous catalysis. First, the nickel is part of a composite (i.e., Ni/YSZ) and the nickel particles have diameters on the order of microns. Also, the temperature is higher in SOFC and the concentration profiles within the anode compartment are different from that in a plug flow reactor because the entrance path for the feed is the same (but in the opposite direction) as the exit path for the products in the anode. There are different strategies to prevent carbon formation in SOFC. Often the feed contains steam to reduce carbon formation but this approach has the disadvantage of reducing the fuel cell electromotive force since water is the product of hydrogen oxidation. Other strategies include the use of materials that reduce the tendency of nickel to produce carbon [30], changing the geometry of the anode with barriers [31] or with bi-layers, and completely replacing the nickel [32,33]. As of yet, these solutions have not produced anodes with comparable properties to Ni/YSZ (activity, ease of manufacture, cost, etc.).

Given the interest in operating SOFC on a variety of fuels, which may consist of mainly CO and H_2 either originally or after gas-phase and/or catalytic reactions in the anode compartment, we have examined the formation of carbon on Ni/YSZ anodes exposed to H_2 and CO mixtures at 1073 K. The electrochemical performance of electrolyte-supported button cells before, during and after exposure to various feeds was determined using electrochemical impedance spectroscopy and cyclic voltammetry. Any carbon formed on the anodes was characterized with temperature-programmed oxidation and the morphology of the anodes was observed with scanning electron microscopy. Differences in the behaviour of the anodes at open circuit potential (OCP) and under polarization were also investigated.

2. Experimental

2.1. Cell preparation and setup

Ni/YSZ anodes were prepared by ball milling equal masses of NiO powder (Alfa Aesar) and YSZ (Tosoh, TZ-8Y) in ethanol for 48 h. The dried powder was then mixed with terpineol (Alfa Aesar) to form a slurry that was painted on the electrolyte and sintered at 1623 K for 2 h. YSZ electrolytes were prepared by pressing YSZ powder into disks and sintering at 1173 K for 4 h. The final thickness of the disks was ~0.5 mm, with an anode thickness of ~25.0 μm. Platinum was used for the cathode and reference electrodes, which were placed on the opposite side of the electrolyte from the anode. Silver loops were used as current collectors. The cell was fixed to the cell holder with glass paste (ESL 4460, The Hydrogen Company, USA) as described in detail elsewhere [29]. The NiO anode was reduced at 1073 K with a stream of 10% H_2 in He for 1 h.

2.2. Electrochemical testing

The anodes were exposed to various CO/H_2 mixtures in ratios of 0/100, 25/75, 50/50, 75/25, and 100/0 (50 mL min^{-1} total flow rate) for 6 h, with a fixed current density of 0 (OCP) or 10 mA cm^{-2} (under polarization). The current density used was very low because the purpose of this study was to evaluate the effect of polarization in a relatively constant bulk gas-phase composition. Testing was performed at a fixed temperature of 1073 K and at atmospheric pressure. All experiments were performed using new cell assemblies and, therefore, some variation of the cell performance is expected due to changes in the microstructure of the electrodes. The OCP with dry H_2 was measured at the beginning of each experiment and then the cells were characterized electrochemically with H_2 before testing with the CO/H_2 mixtures (1287 Potentiostat + 1260 FRA, Solartron Analytical, U.K.). At the beginning ($t = 0$), in the middle ($t = 3$ h) and at the end ($t = 6$ h) of the exposure to the CO/H_2 mixtures, the cell performance was measured using cyclic voltammetry (CV) and electrochemical impedance spectroscopy (EIS). For the CV measurements, the scan rate was 10 mV s^{-1} and the overpotential range was 0–0.5 V. EIS was performed at 0 bias, 10 mV of amplitude and the frequency range was 10^6 to 10^{-2} Hz. After testing, the gas was switched to He and the system cooled. Once at room temperature, the cell was removed from the holder for the characterization of any carbon deposits.

2.3. Characterization

To quantify the amount of carbon deposited on the anodes, temperature-programmed oxidation (TPO) experiments were performed after testing the cells with the CO/H_2 mixtures. For the TPO experiments, a stream of 10% O_2 in He (50 mL min^{-1}) was passed over the sample while the temperature was increased from room temperature to 1173 K at 10 K min^{-1}. The effluent gas was analyzed using a mass spectrometer (Cirrus 200 Quadrupole), and masses 44 (CO_2), 32 (O_2), 28 (CO), 18 (H_2O), and 4 (He) were monitored. The CO_2 signal was calibrated so that the TPO peak area could be converted to the amount of carbon deposited. To study the morphology of the carbon deposited on the anodes, the samples were broken and the cross-sections were observed with a scanning electron microscope (Philips XL30 ESEM). The samples were gold-coated to prevent charging.

3. Results and discussion

3.1. Electrochemical testing

The OCP in dry H_2 varied between 1.16 and 1.25 V for the cells, which corresponds to H_2O concentrations between 1% and 0.1% approximately. Considering that all the conditions (temperature, pressure, gas composition, flow rate, etc.) were the same, this difference in potential is likely due to minor changes in microstructure and/or leaks in the cells. In all cases, the leaks were sufficiently small to not affect the results presented. Fig. 1 shows the EIS results for the cells exposed to different CO/H_2 ratios at OCP and under polarization, after 0, 3 and 6 h. For all CO/H_2 mixtures, the spectra are composed of one arc with, in some cases, a tail at low frequencies. The tail or other artefacts at low frequencies show that the system was not completely stable during the measurements [34,35]. The instability may be caused by changes at the anode surface due to coking or adsorption of other species over the duration of the experiment and, thus, are visible at the lower frequency. In comparison, for dry H_2, the spectra are composed of two semicircles (Fig. 1i), while for humidified H_2, the low frequency arc nearly disappeared and the high frequency arc size decreased (Fig. 1j). The Rs and Rp values are summarized in Table 1.

At $t = 0$, the impedance should be identical for the same gas mixture, whether or not the cell was under polarization. In our results, there is some variation in the initial impedances (Fig. 1 and Table 1). There is no trend for samples at OCP versus under polarization and, thus, these variations are most likely due to preparation variability,

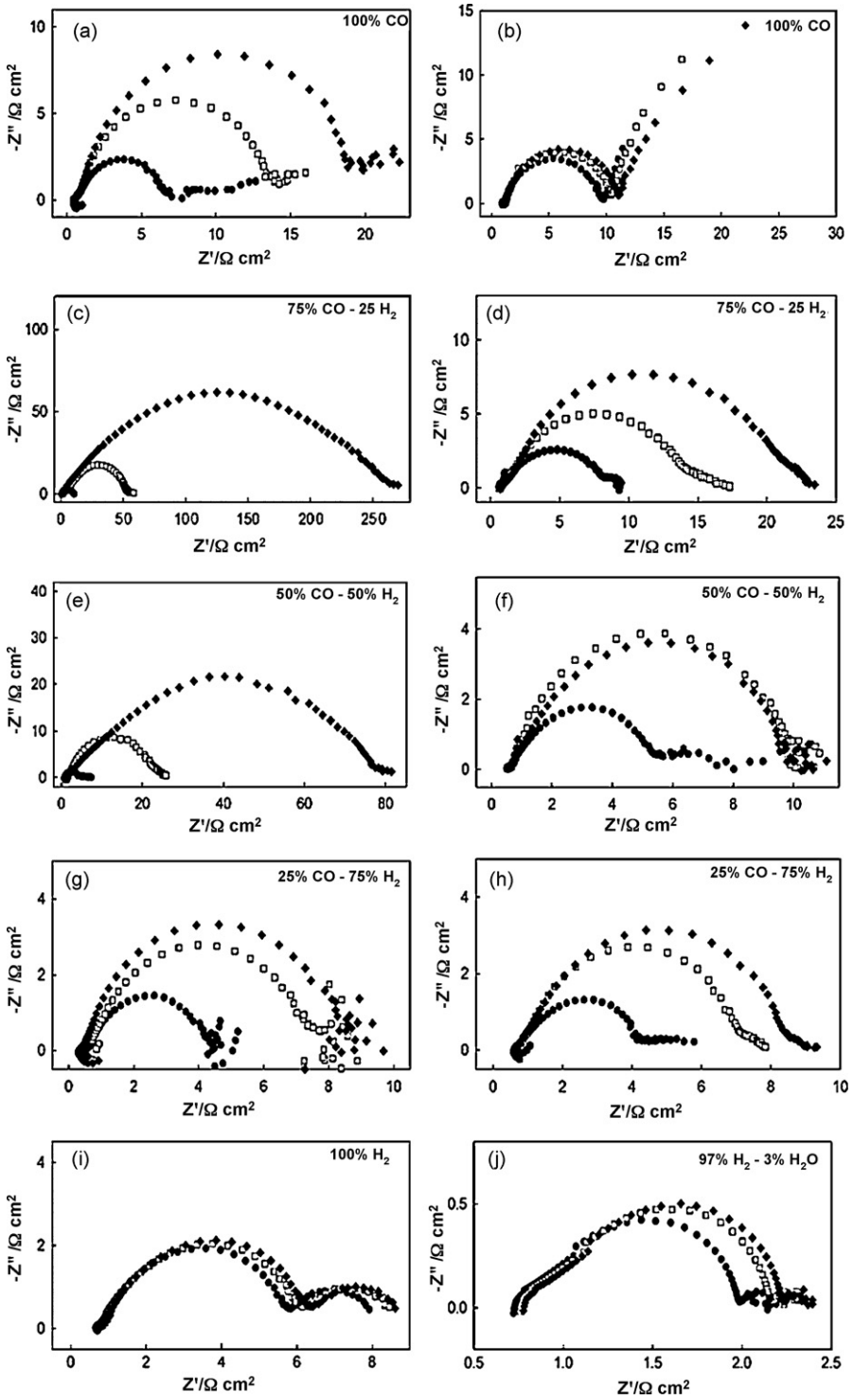

Fig. 1. EIS of Ni/YSZ anodes exposed to different CO/H_2 ratios, after 0 h (●), 3 h (□) and 6 h (◊), at OCP (a, c, e, g, i), under polarization (b, d, f, and h), and humidified hydrogen at OCP (j).

which may have influenced the properties of the cells (e.g., length of the triple phase boundary).

With time, there is an increase in the polarization resistance (Rp) for all cells and this increase is greater at OCP than under polarization (Fig. 1). The cells exposed to dry or humidified H_2 at OCP had relatively stable performance over 6 h (Fig. 1i and j). The relative change in Rp of the other cells was highly dependent on the gas-phase composition and the presence of an applied current. At OCP, the impendence of the cell exposed to 100% CO increased less over 6 h than that of the cells exposed to 75/25 and 50/50 mixtures of CO and H_2 but more than the cell exposed to a 25/75 mixture of CO and H_2. The largest deactivation occurred for the cell exposed to a 75/25 mixture of CO and H_2 at OCP (Fig. 1c) in which Rp increased from 11.3 $\Omega\,cm^2$ to 68.8 $\Omega\,cm^2$ at 3 h and 292 $\Omega\,cm^2$ at 6 h. In contrast, with the same gas mixture (75/25 CO/H_2) but with polarization, Rp increased much less—from 8.39 $\Omega\,cm^2$ to 16.7 $\Omega\,cm^2$ at 3 h and 22.8 $\Omega\,cm^2$ at 6 h (Fig. 1d). With a higher concentration of H_2 in the gas-phase (i.e., 50/50 CO/H_2, Fig. 1e and f), the trends were

Table 1
Summary of electrochemical results.

Gas composition (%CO/%H_2)	Current density (mA cm^{-2})	Voltage (V)	Rs (Ω cm^2)			Rp (Ω cm^2)			Peak frequency (Hz)		
			t = 0	t = 3 h	t = 6 h	t = 0	t = 3 h	t = 6 h	t = 0	t = 3 h	t = 6 h
100/0	0	1.10–1.06	0.48	0.44	0.46	7.2	13	19	10.00	3.162	2.512
75/25	0	1.14–1.13	1.2	1.5	1.2	11	69	290	25.11	19.95	10.00
50/50	0	1.21–1.18	0.68	0.82	1.2	3.5	23	76	31.62	7.943	5.012
25/75	0	1.17	0.52	0.51	0.31	3.9	6.7	7.9	25.11	15.84	10.00
0/100	0	1.22–1.23	0.66	0.71	0.73	5.1	5.6	5.7	19.95	19.95	19.95
0/97 (3%H_2O)	0	1.09	0.72	0.76	0.78	1.3	1.4	1.4	125.9	125.9	125.9
100/0	10	0.95–0.85	0.93	0.91	0.98	8.7	9.6	10	25.11	15.84	15.84
75/25	10	1.08–1.04	0.70	0.60	0.64	8.5	16.7	23	15.84	10.00	6.310
50/50	10	1.10–1.08	0.56	0.48	0.48	4.6	9.1	8.7	19.95	7.943	10.00
25/75	10	1.12–1.11	0.63	0.60	0.59	4.9	7.2	8.7	25.11	12.58	10.00

similar but the increase in Rp with time was less. Interestingly, the impedance spectra were similar for the cells exposed to a 25/75 CO and H_2 mixture at OCP and under polarization (Fig. 1g and h).

The cyclic voltammograms (CVs) measured initially and after 6 h for the cells exposed to 100% CO and 50%CO–50%H_2 at OCP and under polarization are shown in Fig. 2. For each CV, two cycles were measured (each labelled 1 and 2, respectively, in Fig. 2). In the cases where only one CV is visible, the two CVs overlap. Comparing the CVs for 100% CO at OCP at t = 0 h and t = 6 h (Fig. 2a), with time there is a decrease in the slope at low overpotentials, i.e., close to OCP conditions, which might be due to a reduction in the number of active sites due to the deposition of carbon. At high overpotentials, however, the slope increases with time, which is a consequence of a reduction of the ohmic resistance of the cell and suggests that carbon improved the conductivity of the anodes. In the second scan of the CV at t = 6 h, the slope at high overpotentials decreases, which can be explained by the reaction of oxygen ions with the deposited carbon returning the material to its initial conductivity. For the anode exposed to 100% CO under polarization (Fig. 2b), the CVs only show deactivation in the low overpotential region (up to ~0.15 V). For comparison, the maximum current density obtained in H_2 was 0.42 A cm^{-2}.

After exposure to 50%CO–50%H_2 at OCP (Fig. 2c), there is significantly more deactivation with time over the entire overpotential range scanned than for the anodes exposed to 100% CO. Under polarization (Fig. 2d), however, the behaviour of the anode was similar to that of the CVs in Fig. 2a, except that during the second cycle at t = 6 h there is no loss of conductivity. That is, the slope at high overpotentials did not decrease on the second cycle. Since in this case there is H_2 present, the oxygen ions likely preferentially reacted with H_2 rather than with the deposited carbon so there was no change in the conductivity after the first CV cycle.

As seen by the impedance results in Table 1 and the CVs in Fig. 2, the presence of carbon on the anode could either increase or decrease the electrochemical performance of the cell depending on the overpotential. Often the polarization resistance (Rp)

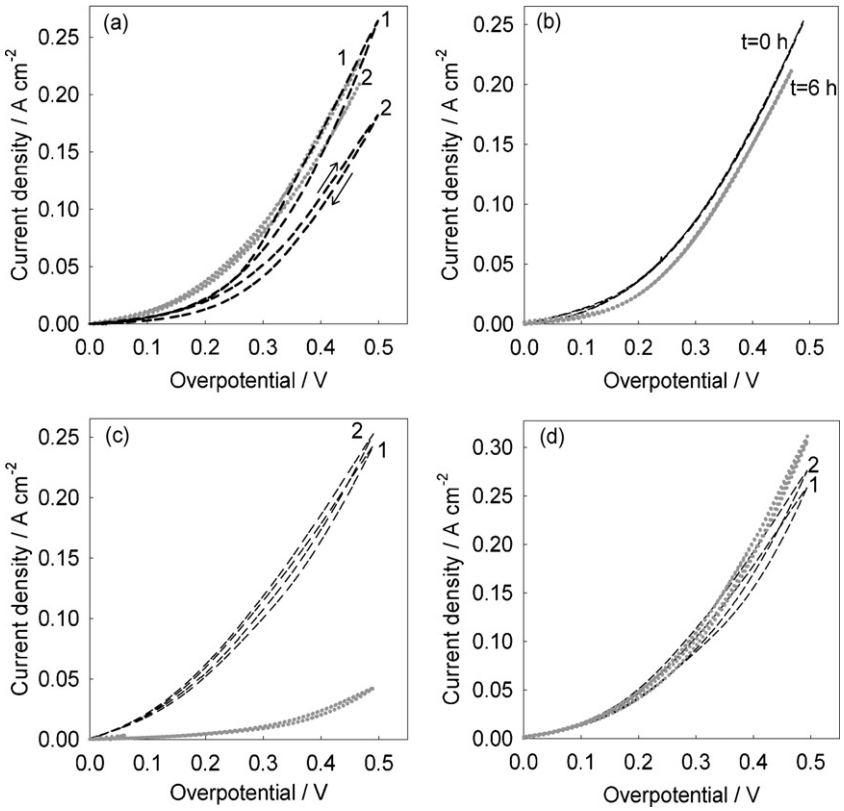

Fig. 2. CVs of Ni/YSZ anodes after 0 h (black, dashed line) and 6 h (gray dotted line), exposed to 100% CO at OCP (a) and under polarization (b), and 50% CO–50% H_2 at OCP (c) and under polarization (d).

increased while the slope at low overpotentials decreased, which is consistent with carbon blocking active sites on the nickel surface. In some cases, however, the cell resistance (Rs) decreased while the slope at high overpotentials increased possibly because the carbon deposits, which are good electron conductors, improved the overall electronic conductivity of the anode.

Weber et al. have reported similar initial cell performances with dry H_2, CO and methane on electrolyte-supported Ni/YSZ anodes at 1223 K [36]. Matsuzaki and Yasuda [37] reported that the rate of the electrochemical oxidation of H_2 is 1.9–2.3 times higher than that of CO at 1023 K as measured in 20% H_2O–80% H_2 and 25% CO_2–75% CO. The results reported here are generally in agreement with these results [36,37]. Specifically, for dry hydrogen the impedance was almost the same as for CO, but the polarization resistance in humidified hydrogen was significantly smaller (Table 1 and Fig. 1). Also there was more deactivation for the anodes exposed to CO and H_2 mixtures (Table 1 and Figs. 1 and 2).

3.2. Carbon deposit characterization

After the anodes were exposed to the CO/H_2 mixtures, the samples were analyzed with temperature-programmed oxidation (TPO) to characterize any deposited carbon. The TPO profiles for the samples operated at OCP are shown in Fig. 3. In all cases, the profiles had single peaks with maximums between 820 and 920 K. CO_2 was the only gas-phase product—no water was evolved from the samples–and, therefore, the deposits consisted of completely dehydrogenated carbon. For the three CO/H_2 mixtures employed in this work, the amount of carbon decreased with increasing hydrogen content, as seen in Fig. 3 and Table 2, while pure CO did not follow this trend. A reduction of more than one order of magnitude in the carbon deposited is achieved by reducing the amount of hydrogen from 25% to 0% in the CO stream. From these results, there is a maximum of carbon deposition between the CO/H_2 ratios of 75/25 and 100/0. The leading edges of the peaks overlap, suggesting that the type of carbon deposited was the same when the anodes were exposed to CO/H_2 mixtures.

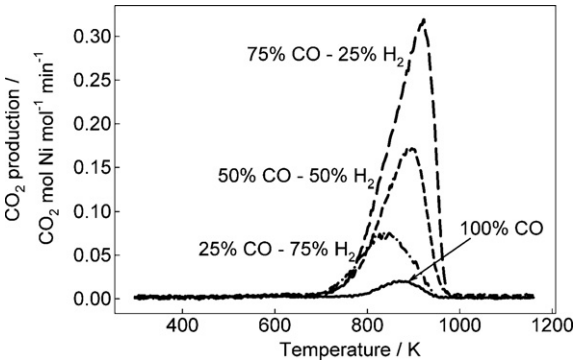

Fig. 3. TPO analysis of Ni/YSZ anodes exposed to CO/H_2 mixtures for 6 h at 1073 K and OCP.

Table 2
Summary of TPO results.

Gas composition (%CO/%H_2)	Current density (mA cm^{-2})	Deposited carbon (Cmol $Nimol^{-1}$)
100/0	0	0.23
75/25	0	3.6
50/50	0	2.0
25/75	0	1.0
100/0	10	0
75/25	10	2.2
50/50	10	1.6
25/75	10	0.88

In Fig. 4, the TPO results presented in Fig. 3 (OCP conditions) are compared with the corresponding TPO profiles for the anodes tested under polarization. In all cases, there is a decrease in the amount of carbon deposited with polarization but the impact of

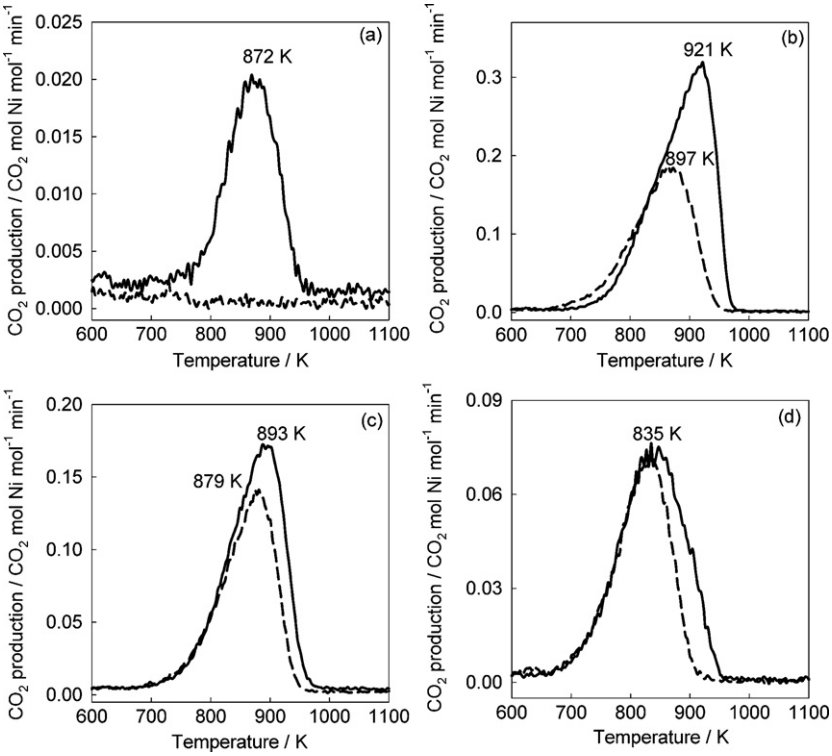

Fig. 4. TPO analysis of Ni/YSZ anodes exposed to: (a) 100% CO, (b) 75% CO–25% H_2, (c) 50% CO–50% H_2, and (d) 25% CO–75% H_2 for 6 h at 1073 K at OCP (solid line) and under polarization (dashed line).

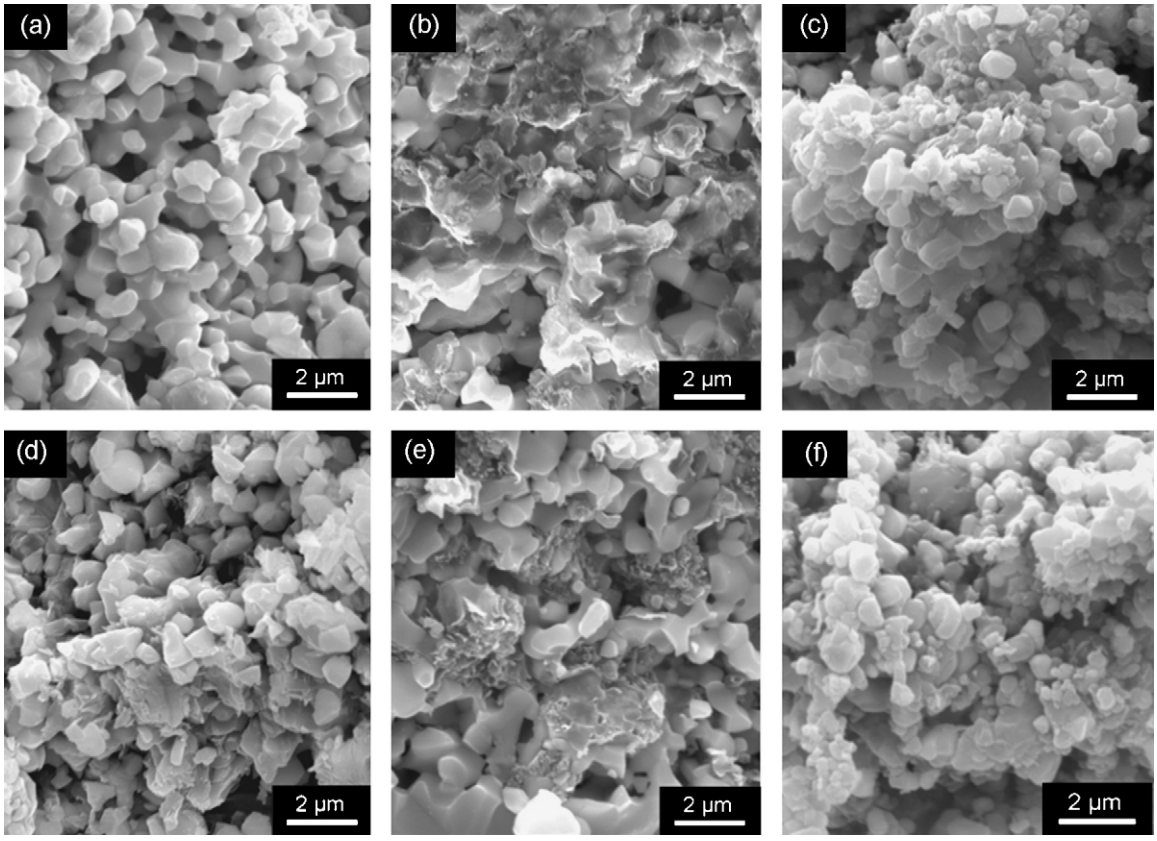

Fig. 5. SEM images of Ni/YSZ anodes exposed to 100% H_2 at OCP (a), 25% CO–75% H_2 at OCP (b), 75% CO–25% H_2 at OCP (c), 100% CO at OCP (d), 25% CO–75% H_2 with 10 mA cm^{-2} (e), and 75% CO–25% H_2 with 10 mA cm^{-2} (f).

polarization depends on the gas composition: the higher the CO content, the greater the decrease in carbon formation with polarization. In fact, there was essentially no carbon formation on the anode exposed to 100% CO for 6 h with 10 mA cm^{-2}, which is consistent with a steady polarization resistance over time (Fig. 1b). Obviously in this situation, electrochemically formed water was not removing the carbon because no hydrogen was present. In comparison, for the anode exposed to the mixture of 25%CO–75%H_2 (Fig. 4d), there was only a 12% reduction in the amount of carbon deposited. The anodes exposed to the other two gas compositions, 50%CO–50%H_2 and 75%CO–25%H_2, decreased their carbon deposits by 20% and 39%, respectively. These decreases are consistent with the corresponding changes in the polarization resistances (Fig. 1 and Table 1). There was little change in the peak positions indicating that the type of carbon formed under polarization did not change from that formed at OCP.

The SEM images of anodes exposed to H_2/CO mixtures are shown in Fig. 5. The image of the anode exposed to H_2 (Fig. 5a) is identical to the image of an as-prepared sample and the anode exposed to 100% CO under polarization. Thus, any changes to the morphologies of the other anodes were due to carbon deposition. The Ni/YSZ anodes had a relatively homogeneous structure in terms of particle size and porosity as seen in Fig. 5a. After exposure to CO or CO/H_2 mixtures at OCP, the anodes have reduced porosities (Fig. 5b–d). In all cases, the carbon has dissolved into and swollen the Ni particles. The anode exposed to 25%CO–75%H_2 under polarization (Fig. 5e) does not appear to be that different from the anode exposed to the same gas mixture at OCP (Fig. 5b), which is consistent with similar amounts of carbon being deposited on the anodes in each case (Fig. 4d).

There was a larger difference in the amount of carbon deposited for the anodes exposed to 75%CO–25%H_2 with and without polarization (Fig. 4b) but the SEM images (Fig. 5c and f, respectively) are similar. On a larger scale (Fig. 6), however, the samples are very different. While the anode under polarization remained intact (Fig. 6a), the anode exposed to 75%CO–25%H_2 at OCP

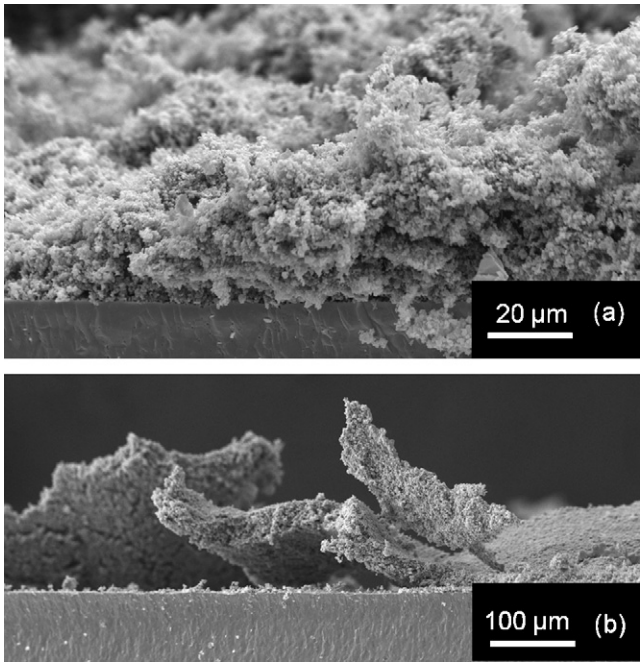

Fig. 6. SEM images of Ni/YSZ anodes exposed to 75% CO–25% H_2: (a) with 10 mA cm^{-2} and (b) at OCP.

delaminated from the electrolyte, which is consistent with the significant increase in the polarization resistance (Fig. 1c). This sample did not break cleanly, when exposing the cross-section, like the other samples but rather fell apart when handled. The deposited carbon obviously destroyed the structure of the Ni/YSZ anode.

3.3. Discussion

Although the amount of carbon deposited on the anodes was not large at the conditions of this study (Figs. 3 and 4), it was sufficient to hinder the electrochemical performance (Figs. 1 and 2), and in one case (75%CO–25%H_2 at OCP) resulted in the delamination of the cell (Fig. 5). As mentioned, the Ni/YSZ structure was very fragile after exposure to 75%CO–25%H_2 compared to the other anodes. Work done by Chun et al. [28] compared the morphology of carbon deposited on Ni foils with CO/H_2 ratios of 25 and 1. They suggested that for high concentrations of CO there is a loss of Ni content due to intercalation with surface graphite; while for a CO/H_2 ratio of one there is also the diffusion of carbon into the bulk of the nickel causing the expansion of the material as graphite precipitates in the bulk of the nickel, and the material bursts and disintegrates [28]. Nolan et al. proposed that CO would form "closed forms" of carbon structures, like shells and nanotubes, while CO/H_2 mixtures would form "open forms" like filaments [38–40] at temperatures between 673 and 773 K. The open forms of carbon can continue to grow indefinitely as the catalytic site is always accessible.

From the SEM images in this study, it appears that the carbon may have diffused into the nickel particles resulting in swelling and a subsequent reduction in the porosity of the anode. Changes in the surface morphology of the particles can be interpreted as blocking of active sites by the carbon deposits. Carbon may be formed from the disproportionation reaction (Eq. (4)) or CO reduction (Eq. (5)). It was surprising that more carbon was deposited from the CO/H_2 mixtures than from pure CO. In the metal dusting literature, CO reduction has been suggested to be a more important reaction than CO disproportionation, in terms of carbon deposition processes on transition metals at intermediate to high temperatures (673–1073 K) [41]. At 953 K, CO reduction and CO disproportionation are kinetically limited from reaching equilibrium but the rate constant for the former reaction is 10 times higher than for the latter reaction—$k = 0.73\ \mathrm{mg\,cm^{-2}\,atm^{-2}\,h^{-1}}$ for reduction versus $k = 0.06\ \mathrm{mg\,cm^{-2}\,atm^{-2}\,h^{-1}}$ for disproportionation over a Ni foil [18].

The mechanism of carbon formation from CO/H_2 mixtures is not fully understood but may be related to reverse gasification processes [41], hydrogen removing the adsorbed oxygen species to free up surface sites, and/or hydrogen assisting the decomposition of CO [42]. Theoretical calculations [43] suggest that addition of atomic hydrogen to adsorbed CO, forming a formyl intermediate, is a first elementary step preceding that of breaking the C–O bond in Fischer–Tropsch synthesis; the H-assisted CO dissociation route is more facile than the direct C–O bond scission in adsorbed CO. This mechanism would be consistent with the results obtained in this study (Figs. 3 and 4) in which significantly more carbon was deposited on the Ni/YSZ exposed to CO/H_2 mixtures than to pure CO.

When the cells were operated under an applied potential, less carbon was formed, and in the case of a pure CO feed, no carbon was formed. This result has the practical application of potentially being able to operate a SOFC directly on a CO feed, although there may still be carbon formation in the conduction layer of an anode-supported cell. In this study, the anode thickness was ~25 μm and so most of the Ni was in the functional layer and participating in the electrochemical reaction. As no hydrogen was present, the lack of carbon formation under an applied potential was not a result of water production at the anode.

The electrochemical oxidation of hydrogen is faster than the electrochemical oxidation of CO [37], and the rates of these reactions depend on the partial pressure of the reactants. Hence, for the case where there is a high partial pressure of hydrogen it would be expected that the oxidation of hydrogen would take place preferentially over the oxidation of CO. The formation of water could have removed some of the deposited carbon, although the production of water was small because of the low current density ($10\ \mathrm{mA\,cm^{-2}}$) used. The results, however, indicate that the presence of water had essentially no effect because applied potential had less effect on carbon deposition as the concentration of H_2 in the feed was increased (Fig. 3). If water was a factor in reducing carbon deposition, the opposite trend would have been observed.

In comparison with previous TPO experiments on anodes exposed to methane at the same current density [29], polarization had a much greater effect on reducing carbon deposition for methane. Specifically, for anodes exposed to methane, TPO peak temperatures were shifted lower by approximately 200 K, the amount of carbon deposited was decreased by an order of magnitude, and the carbon deposits contained some hydrogen (that is, an H_2O peak accompanied the CO_2 peak in the TPO analysis) with the addition of polarization. These results are consistent with the electrochemical reactions impacting the last dehydrogenation step of adsorbed methane. The mechanism of carbon formation and removal is clearly different for methane than for CO/H_2 mixtures and will be investigated in more detail in future experiments.

4. Conclusions

The behaviour of electrolyte-supported Ni/YSZ anodes exposed to CO/H_2 mixtures at 1073 K and OCP or with a current density of $10\ \mathrm{mA\,cm^{-2}}$ has been investigated in this study. In general, carbon formation occurred over time and deactivated the anodes by increasing the polarization resistance, reducing porosity and blocking active sites. In the worst case, an anode exposed to 75%–25% CO/H_2 at OCP delaminated after 6 h of operation. In the best case, an anode exposed to 100% CO with a current density of $10\ \mathrm{mA\,cm^{-2}}$ had stable performance with no carbon formation over 6 h. Although it was expected that the presence of H_2 would reduce the amount of carbon formation, there was actually more carbon deposited on the anodes exposed at OCP to the feeds containing CO/H_2 mixtures (in the ratios of 75/25, 50/50 and 25/75) than to pure CO. Polarization reduced the amount of carbon formation—completely for a feed of 100% CO and between 12% and 39% for the CO/H_2 mixtures.

Acknowledgements

This research was supported through funding to the NSERC Solid Oxide Fuel Cell Canada Strategic Research Network from the Natural Science and Engineering Research Council (NSERC) and other sponsors listed at www.sofccanada.com. We thank Dr. Charles Mims for helpful discussions.

References

[1] R.M. Ormerod, in: S.C. Singhal, K. Kendall (Eds.), High Temperature Fuel Cells: Fundamentals, Design and Applications, Elsevier, 2003, pp. 333–361.
[2] M. Cimenti, J.M. Hill, J. Power Sources 186 (2009) 377–386.
[3] R.S. Gemmen, J. Trembly, J. Power Sources 161 (2006) 1084–1095.
[4] A.O. Omosun, A. Bauen, N.P. Brandon, C.S. Adjiman, D. Hart, J. Power Sources 131 (2004) 96–106.
[5] C.H. Bartholomew, Catal. Rev.-Sci. Eng. 24 (1982) 67–112.
[6] H.S. Bengaard, J.K. Norskov, J. Sehested, B.S. Clausen, L.P. Nielsen, A.M. Molenbroek, J.R. Rostrup-Nielsen, J. Catal. 209 (2002) 365.
[7] H. He, J.M. Hill, Appl. Catal., A 317 (2007) 284.

[8] I. Alstrup, M.T. Tavares, C.A. Bernardo, O. Sorensen, J.R. Rostrup-Nielsen, Mater. Corros. 49 (1998) 367–372.
[9] R.T.K. Baker, Carbon 27 (1989) 315–323.
[10] S. Helveg, C. Lopez-Cartes, J. Sehested, P.L. Hansen, B.S. Clausen, J.R. Rostrup-Nielsen, F. Abild-Pedersen, J.K. Norskov, Nature 427 (2004) 426–429.
[11] C.W. Keep, R.T.K. Baker, J.A. France, J. Catal. 47 (1977) 232–238.
[12] P.G. Menon, J. Mol. Catal. 59 (1990) 207–220.
[13] G.D. Renshaw, C. Roscoe, P.L. Walker J., J. Catal. 22 (1971) 394–410.
[14] J. Rostrup-Nielsen, D.L. Trimm, J. Catal. 48 (1977) 155–165.
[15] J.R. Rostrup-Nielsen, J. Catal. 27 (1972) 343–356.
[16] D.L. Trimm, Catal. Rev.-Sci. Eng. 16 (1977) 155–189.
[17] J. Zhang, P. Munroe, D.J. Young, Acta Mater. 56 (2008) 68.
[18] J. Zhang, D.J. Young, Corros. Sci. 49 (2007) 1496.
[19] A.S. Ferlauto, D.Z. De Florio, F.C. Fonseca, V. Esposito, R. Muccillo, E. Traversa, L.O. Ladeira, Appl. Phys. A: Mater. Sci. Process. 84 (2006) 271–276.
[20] J.W. Snoeck, G.F. Froment, M. Fowles, J. Catal. 169 (1997) 240–249.
[21] H.J. Grabke, R. Krajak, J.C.N. Paz, Corros. Sci. 35 (1993) 1141–1150.
[22] D. Singh, E. Hernandez-Pacheco, P.N. Hutton, N. Patel, M.D. Mann, J. Power Sources 142 (2005) 194–199.
[23] K. Nikooyeh, R. Clemmer, V. Alzate-Restrepo, J.M. Hill, Appl. Catal., A 347 (2008) 106–111.
[24] S. McIntosh, H.P. He, S.I. Lee, O. Costa-Nunes, V.V. Krishnan, J.M. Vohs, R.J. Gorte, J. Electrochem. Soc. 151 (2004) A604–A608.
[25] J. Macek, B. Novosel, M. Marinnsek, J. Eur. Ceram. Soc. 27 (2007) 487–491.
[26] T. Kim, G. Liu, M. Boaro, S.I. Lee, J.M. Vohs, R.J. Gorte, O.H. Al-Madhi, B.O. Dabbousi, J. Power Sources 155 (2006) 231–238.
[27] T. Horita, K. Yamaji, T. Kato, H. Kishimoto, Y.P. Xiong, N. Sakai, M.E. Brito, H. Yokokawa, J. Power Sources 145 (2005) 133–138.
[28] C.M. Chun, J.D. Mumford, T.A. Ramanarayanan, J. Electrochem. Soc. 147 (2000) 3680–3686.
[29] V. Alzate-Restrepo, J.M. Hill, Appl. Catal., A 342 (2008) 49–55.
[30] M. Boder, R. Dittmeyer, J. Power Sources 155 (2006) 13–22.
[31] H.Y. Zhu, A.M. Colclasure, R.J. Kee, Y.B. Lin, S.A. Barnett, J. Power Sources 161 (2006) 413–419.
[32] A. Atkinson, S. Barnett, R.J. Gorte, J.T.S. Irvine, A.J. McEvoy, M. Mogensen, S.C. Singhal, J. Vohs, Nat. Mater. 3 (2004) 17–27.
[33] Y. Zheng, W. Zhou, R. Ran, Z.P. Shao, Prog. Chem. 20 (2008) 413–421.
[34] J.R. Macdonald, Impedance Spectroscopy, John Wiley & Sons, New York, 1987.
[35] J.H. Koh, Y.S. Yoo, J.W. Park, H.C. Lim, Solid State Ionics 149 (2002) 157–166.
[36] A. Weber, B. Sauer, A.C. Muller, D. Herbstritt, E. Ivers-Tiffee, Solid State Ionics 152 (2002) 543–550.
[37] Y. Matsuzaki, I. Yasuda, J. Electrochem. Soc. 147 (2000) 1630–1635.
[38] P.E. Nolan, D.C. Lynch, A.H. Cutler, Carbon 32 (1994) 477–483.
[39] P.E. Nolan, D.C. Lynch, A.H. Cutler, Carbon 34 (1996) 817–819.
[40] P.E. Nolan, M.J. Schabel, D.C. Lynch, A.H. Cutler, Carbon 33 (1995) 79–85.
[41] C.R.F. Lund, J. Catal. 95 (1985) 71–83.
[42] X. Dai, C. Yu, J. Nat. Gas Chem. 17 (2008) 365–368.
[43] M. Mavrikakis, Private communication (2009).